

# Exploring plasma evolution during Sagittarius A\* flares

S. Dibi<sup>1</sup>, S. Markoff<sup>1</sup>, R. Belmont<sup>2,3</sup>, J. Malzac<sup>2,3</sup>, N. M. Barrière<sup>4</sup>  
and J. A. Tomsick<sup>4</sup>

<sup>1</sup>Astronomical Institute “Anton Pannekoek”, University of Amsterdam, Postbus 94249, 1090  
GE Amsterdam, The Netherlands  
email: s.dibi@uva.nl

<sup>2</sup>Université de Toulouse; UPS-OMP; IRAP; Toulouse, France

<sup>3</sup>CNRS; IRAP; 9 Av. colonel Roche, BP 44346, F-31028 Toulouse cedex 4, France

<sup>4</sup>Space Sciences Laboratory, 7 Gauss Way, University of California, Berkeley, CA 94720, USA

**Abstract.** We present a new way of describing the flares occurring from Sgr A\* within a single zone with a self-consistent calculation of the particle distribution. The results allow us to give an interpretation to the flaring events generated very close to the supermassive black hole (SMBH) without assuming a specific particle distribution. We conclude that the flare data are more likely generated by a weakly magnetized plasma in which the particles flow in and out as expected from an accretion flow. Such a plasma, with prescription for non-thermal acceleration, injection, escape, and cooling losses, gives a spectrum with a break between the infra-red and the X-ray, allowing a better simultaneous match in the different wavelengths. The parameters favor the non-thermal synchrotron spectrum, and a decrease/increase of the magnetic field and plasma density are not favored for producing the flare event, but particle acceleration must be happening by other means. We show that under certain conditions, the real particle distribution can differ significantly from the standard distributions used in such studies.

**Keywords.** Galaxy: center — Galaxy: nucleus, accretion disks, black hole physics — MHD — radiation mechanisms — relativistic processes — methods: numerical.

---

## 1. Introduction

Sgr A\* is one of the most under-luminous SMBHs that we know, with  $L_{\text{bol}} \simeq 10^{-9} L_{\text{Edd}}$ , and it is accreting at a very low rate ( $2 \times 10^{-9} < \dot{M} < 2 \times 10^{-7} M_{\odot} \text{yr}^{-1}$ ; Bower *et al.* 2003; Marrone *et al.* 2007). Theoretical work suggest also that Sgr A\* is most likely accreting at the lower range of this interval, with a weakly magnetized ( $\lesssim$  few hundred Gauss) and faint ( $\rho \lesssim 10^8 \text{ cm}^{-3}$ ) plasma (Mościbrodzka *et al.* 2009; Dexter *et al.* 2009; Dibi *et al.* 2012; Drappeau *et al.* 2013).

The faint emission from Sgr A\* has been observed in different wavelengths giving us a broad band spectrum of this object from the radio to the X-ray (see reviews by Genzel *et al.* 2010; Morris *et al.* 2012, and references therein). The radio wavelength, as well as the quiescent X-ray emission are coming from extended regions around Sgr A\* that we are not modeling here, while the sub-mm, NIR, and flaring X-ray emissions originate from a region very close to the SMBH that we focus on. The fast variability indicates that the origin of the flares is as close as a few gravitational radii from the SMBH. However, the nature of the physical processes responsible for the flares is still an open question. Different mechanisms have been proposed such as magnetic reconnection, infall of gas clumps, disruptions of small bodies, adiabatic expansion of hot plasma or other acceleration processes and several studies have been devoted to the modeling of Sgr A\*

flares. Some models include a precise description of the flow geometry (Yuan *et al.* 2003). However, even in models where the geometry is dealt with accuracy, most of the emission originates from the very central parts of the accretion flow, both in the quiescent sub-mm and NIR bands, and in the flaring sub-mm to X-ray bands. Therefore, most attempts to model the sub-mm to X-ray spectrum of Sgr A\* in the quiescent and flaring states (excluding the radio emission) implicitly assume that the emission originates from a single homogeneous, isotropic zone characterized by only few parameters such as the average electron temperature and density and the magnetic field intensity (e.g. Dodds-Eden *et al.* 2010; Liu *et al.* 2006). Here we use the same approach. The emitted spectrum depends drastically on the particle distribution. For the sake of simplicity, all models so far have assumed pre-determined particle distributions (Maxwellian, power-law, broken power-law, or combinations of them), which are described by few parameters. The precise shapes of the particle distributions depend on the radiative and acceleration processes and can deviate significantly from the assumed ones. The present work aims at dealing more precisely with particle distributions.

## 2. Method

We use the BELM code (Belmont *et al.* 2008). This numerical tool solves simultaneously coupled kinetic equations for leptons and photons in a magnetized, uniform, isotropic medium of typical size  $R$ . In all models presented here, this size is set to  $R = 2 r_G = 1.3 \times 10^{12}$  cm based on the size derived from the flare time scale variability. The implemented microphysics includes radiation processes such as self-absorbed radiation, Compton scattering, self-absorbed bremsstrahlung radiation, pair production/annihilation, Coulomb collisions, and prescriptions for particle heating/acceleration. We use two different channels to provide energy to the particles: 1) We mimic thermal processes by computing Coulomb collisions with a virtual population of hot protons (with temperature  $k_B T_p = 40$  MeV). This prescription aims at reproducing the effect of anomalous processes (such as viscosity) on the lepton distribution. This free parameter is described by the compactness parameter  $l_{\text{th}} = \sigma_T L_{\text{th}} / (R m_e c^3)$ . Such a prescription not only heats the global distribution of particles, it also thermalizes it. 2) We model non-thermal processes by taking particles from the lepton population itself and re-distribute them as a power-law shape  $N(\gamma) \propto \gamma^{-s}$ . This prescribed distribution for acceleration is characterized by 4 parameters: the slope  $s$ , the minimal and maximal energies  $\gamma_{\text{min}}$  and  $\gamma_{\text{max}}$  respectively, and the normalization. The minimal energy of the power-law will be set to  $\gamma_{\text{min}} = 50$ , so that particles are accelerated from the bulk of the distribution (the thermal peak of the Sgr A\* spectrum implies an electron temperature around  $10^{11}$  K). And the maximal energy of accelerated particles is set to  $\gamma_{\text{max}} = 10^6$ , large enough so that our results do not depend on this parameter, motivated by the facts that a high energy cutoff has not been detected from NuSTAR observations (Barrière *et al.*, submitted), and the possible physical processes responsible for the non-thermal component can accelerate electrons to very high energies. The normalization is computed so that the non-thermal process injects into the region a power  $L_{\text{nth}}$  (erg/s), described by the free parameter  $l_{\text{nth}} = \sigma_T L_{\text{nth}} / (R m_e c^3)$ .

Such prescriptions compete with all other processes to produce complex distributions of particles.

## 3. Modeling the particle dynamics

In the first configuration, we consider a closed region characterized by 5 free parameters: the lepton density  $n_e$ , the magnetic field, the power of the thermal heating and

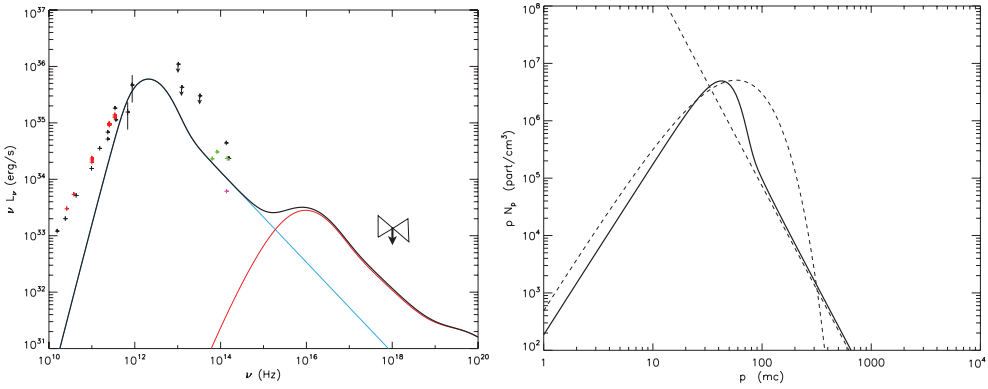


**Figure 1.** Quiescent spectrum from Sgr A\* (**left panel**) and the associated lepton distribution (**right panel**) in a closed system configuration. For a description of the different data points, see Dibi *et al.* (submitted to MNRAS). The calculated spectrum is dominated by synchrotron process, and synchrotron self Compton from a model with  $\rho \simeq 4.6 \times 10^6 \text{ cm}^{-3}$ , and  $B \simeq 150$  Gauss. On the electron distribution (**right panel**), the solid line is the shape of the calculated distribution from which the spectrum comes from, while the dotted lines indicate a pure Maxwellian plus power-law component for comparison. We can notice in this case a significant deviation. [A COLOR VERSION IS AVAILABLE ONLINE.]

non-thermal acceleration characterized by the compactness parameters  $l_{th}$  and  $l_{nth}$  respectively, with the slope for the non-thermal heating process  $s$ . In this model without particle escape, the particle distribution results from the balance between thermal heating, non-thermal acceleration, and radiative cooling.

In the second configuration particles enter the system and can escape. This model is described by four free parameters: the magnetic field, the non thermal compactness  $l_{nth}$  with the slope  $s$ , and the injection compactness  $l_{inj}$ . We consider that injected particles are thermal (coming from the accretion disk). In this case, the particle density is no longer a free parameter and results from the balance between injection and escape.

Figure 1 shows a possible spectrum for Sgr A\* when it is not flaring. The quiescent spectrum can also be obtained with the assumption that particles flow in and out of the emitting region (second configuration), in this case the spectrum is similar to that in Figure 1 but with a slightly larger luminosity in the X-ray. The resulting density is then  $\rho \simeq 3.5 \times 10^7$ , with the parameters  $B \simeq 50$ ,  $l_{nth} = 1 \times 10^{-4}$ ,  $s = 3.6$ ,  $l_{inj} = 5 \times 10^{-3}$ .

In order to get Compton emission for the X-ray flare (see Dibi *et al.* submitted to MNRAS, for a figure and more details), the magnetic field decreases, the non-thermal heating parameter  $l_{nth}$  is more than an order of magnitude higher than in the quiescent state, and the amount of injected particles is also higher leading to a high density reaching the upper limit of  $10^8$  particles per cubic centimeter.

In the case of a flare spectrum dominated by synchrotron emission as seen in Figure 2, only the non-thermal component is modified: the heating parameter  $l_{nth}$  is increasing by a factor six, and the slope becomes flatter (from 3.6 to 2.6) during the flare, meaning that we have more particles in the higher energy part of the electron distribution. So, we must have some physical processes that accelerate the particles more efficiently in the flaring state and that creates a harder non-thermal distribution.

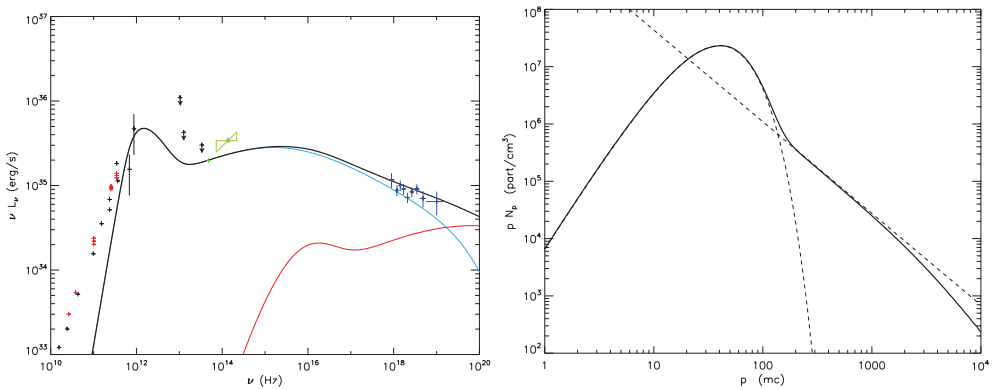


**Figure 2.** Flare spectrum from Sgr A\* (**left panel**) and the associated lepton distribution (**right panel**) in the open configuration (injection of particles and escape). For a description of the different data points, see Dibi *et al.* (submitted to MNRAS). The “bowtie” is one of the only slope that has been observed so far in the IR. The X-ray data points is a flare observed with *NuSTAR* on July 21st 2012. (Barrière *et al.* submitted). The calculated electron distribution (full line) and the theoretical one (dotted line) as a comparison. [A COLOR VERSION IS AVAILABLE ONLINE.]

#### 4. Conclusions

The best model for the flaring state of Sgr A\* is the one shown on Figure 2 because the trends of the multi-wavelength data are better reproduced and few parameters need to be adjusted in order to move from the quiescent to the flaring state. This is especially true if we consider that the green “bowtie” is a typical IR slope. Our conclusions are in good agreement with Dodds-Eden *et al.* (2010) who also favor non-thermal synchrotron processes and a cooling break in order to explain the observed IR and X-ray flares. However, in our study we do not make the hypothesis of magnetic reconnection as an energy source for the flares, and our conclusions do not favor this particular process. In our best case scenario, the magnetic field is not dropping. A decrease of the magnetic field has important consequences on the sub-millimeter and thermal part of the spectrum that we also model here, other parameters have then to be carefully adjusted in order to maintain the sub-mm spectrum, so we think other acceleration mechanisms are more likely to be happening. Reconnection mechanisms could also occur in very localized regions, and particles would diffuse away from the reconnection sites and radiate in a field which has not reconnected, so we would not notice any significant global drop of the magnetic field amplitude.

#### References

- Belmont, R., Malzac, J., & Marcowith, A. 2008, *A&A* 491, 617  
 Bower, G. C., Wright, M. C. H., Falcke, H., & Backer, D. C. 2003, *ApJ* 588, 331  
 Dexter, J., Agol, E., & Fragile, P. C. 2009, *ApJ Lett.* 703, L142  
 Dibi, S., Drappeau, S., Fragile, P. C., Markoff, S., & Dexter, J., 2012, *MNRAS* 426, 1928  
 Dodds-Eden, K., Sharma, P., Quataert, E., Genzel, R., Gillessen, S., Eisenhauer, F., & Porquet, D. 2010, *ApJ* 725, 450  
 Drappeau, S., Dibi, S., Dexter, J., Markoff, S., & Fragile, P. C., 2013, *MNRAS* 431, 2872  
 Genzel, R., Eisenhauer, F., & Gillessen, S. 2010, *Reviews of Modern Physics*, 82, 3121  
 Liu, S., Petrosian, V., Melia, F., & Fryer, C. L. 2006, *ApJ* 648, 1020

- Marrone, D. P., Moran, J. M., Zhao, J.-H., & Rao, R. 2007, *ApJ Lett.* 654, L57
- Morris, M. R., Meyer, L., & Ghez, A. M. 2012, *Research in Astronomy and Astrophysics*, 12, 995
- Mościbrodzka, M., Gammie, C. F., Dolence, J. C., Shiokawa, H., & Leung, P. K. 2009, *ApJ* 706, 497
- Yuan, F., Quataert, E., & Narayan, R. 2003, *ApJ* 598, 301